

Unusual elastic constants of cubic MnTe in strained-layer superlattices measured by x-ray diffraction

J. R. Buschert and F. C. Peiris

Turner Laboratory, Department of Physics, Goshen College, Goshen, Indiana 46526

N. Samarth,* H. Luo, and J. K. Furdyna

Department of Physics, University of Notre Dame, Notre Dame, Indiana 46556

(Received 27 October 1992; revised manuscript received 5 November 1993)

Elastic constants of the recently grown nonequilibrium zinc-blende form of MnTe were measured. Strained layer MnTe/ZnTe superlattices in which MnTe appears in this zinc-blende form were studied using triple crystal x-ray diffraction. The diffraction spectra were fitted using a dynamical model to determine the thickness and the lattice constants of each layer. From these and other measurements, the elastic constants C_{11} and C_{12} of MnTe were determined to be 2.22 ± 0.1 and 1.16 ± 0.1 , respectively. These values are very low compared to all other zinc-blende or diamond structure materials investigated so far.

INTRODUCTION

Because molecular-beam-epitaxy (MBE) growth occurs far from equilibrium it can be used to produce metastable structures.¹ Pure MnTe, which has a hexagonal NiAs structure in bulk form, can be grown in the zinc-blende structure by MBE on zinc-blende substrates. The band gap of MnTe changes from its hexagonal form value of 1.3 to 3.2 eV in the zinc-blende form² and is therefore useful in producing wide-gap barriers in quantum structures. The knowledge of the elastic constants of this new phase of MnTe will facilitate the fabrication of these layered structures. However, these values have not previously been determined.

Although there is about 4% lattice mismatch between MnTe and ZnTe, if the thickness of the individual layers is kept below a critical value, a strained layer superlattice (SLS) (Refs. 3 and 4) can be formed in which the layers are strained but pseudomorphic. In such a MnTe/ZnTe SLS, MnTe appears in the zinc-blende structure and also is strained. So by measuring these strains, it is possible to calculate the elastic constants of this new phase of MnTe.

In this case the ordinary double crystal x-ray-diffraction geometry is inadequate for analyzing superlattices. Because of the presence of a mosaic structure in the samples, the satellite peaks become indistinguishable with this method. The triple crystal diffraction^{5,6} geometry is an ideal method that can resolve these satellite peaks.

While simple x-ray lattice-parameter measurements have already been made on this new zinc-blende phase of MnTe by others,² we undertook a more detailed study of lattice parameter, perfection, and determination of the elastic constants of this new material.

EXPERIMENTAL DESCRIPTION

Sample *A* was a 1.5- μm layer of MnTe grown on a ZnTe buffer and a GaAs substrate. Samples *B* and *C*

were MnTe/ZnTe superlattices grown on a ZnTe buffer and a GaAs substrate. All three samples were grown using a Riber MBE 32 R&D system. The GaAs substrates were commercially polished (100) wafers which were 2–3 cm^2 in area. The substrate temperature during growth was 320 °C and the ZnTe buffer thickness was about 5000 Å in all of the samples. The growth rates of ZnTe and MnTe were 2 and 1.5 Å/s, respectively. Growth interruption of 2 s was used between the ZnTe and the MnTe growth cycles to lessen the possibility of interdiffusion. TEM results showed the formation of coherent superlattice structures with sharp interfaces.

Sample *A* was used to determine the lattice parameter of zinc-blende MnTe using a powder diffractometer. Samples *B* and *C* were analyzed using a triple crystal arrangement. A standard molybdenum x-ray tube was used with two (400) germanium crystals placed as the monochromator and the analyzer.

RESULTS

From the experiment performed on sample *A* the natural lattice parameter of zinc-blende MnTe was determined to be 6.343 Å. This is in excellent agreement with the extrapolated value of 6.34 Å achieved through the work done on zinc-blende alloys of $\text{Zn}_x\text{Mn}_{1-x}\text{Te}$, $\text{Cd}_x\text{Mn}_{1-x}\text{Te}$, and $\text{Hg}_x\text{Mn}_{1-x}\text{Te}$ (Ref. 7) (Fig. 1). Previous experimental work had determined a value of 6.33 Å (Ref. 2).

The θ - 2θ experimental scan of sample *B* and a calculated curve are shown in Fig. 2. The width [full width at half maximum (FWHM)] of the superlattice peaks in the triple crystal scan was about 300 arc sec. Since this type of scan is insensitive to the mosaic spread in the sample it only reveals the variation in the superlattice period which is 0.74%.

A triple crystal rocking scan (equivalent to a transverse scan in q space) performed on the second superlattice peak had a FWHM of 790 arc sec. This type of scan in

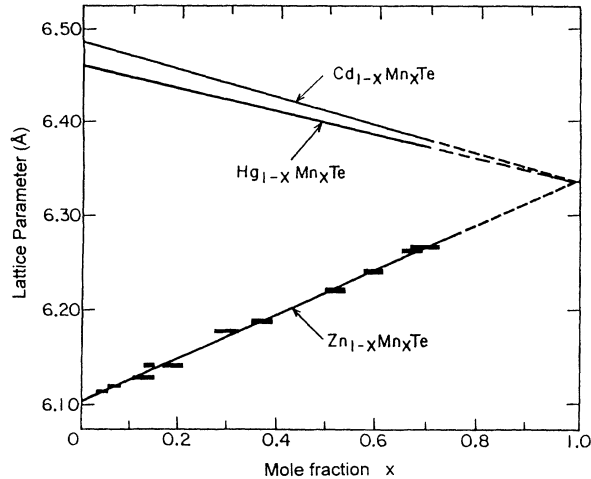


FIG. 1. Lattice parameter as a function of Mn mole fraction x . The extrapolated lines converge at 6.34 \AA , which determines the lattice parameter for the zinc-blende phase of MnTe (after Ref. 15).

the triple crystal arrangement is a pure measure of the mosaic spread of the superlattice, being completely insensitive to variations in the superlattice period. This is a measure of the "waviness" in the boundaries of the layers in the superlattice, not necessarily the atomic planes.

To extract information about the layer thickness and strains, an approach developed by Berreman⁸ was used. This method is a dynamical theory and is especially well suited for layered structures. It uses Abeles's matrix method⁹ for computing optical reflectivity of multilayered structures.

Though the samples were composed of 100 periods, the best fits were achieved using only about three periods. Even then the peak widths were somewhat narrower than the experimental data, suggesting that the structures

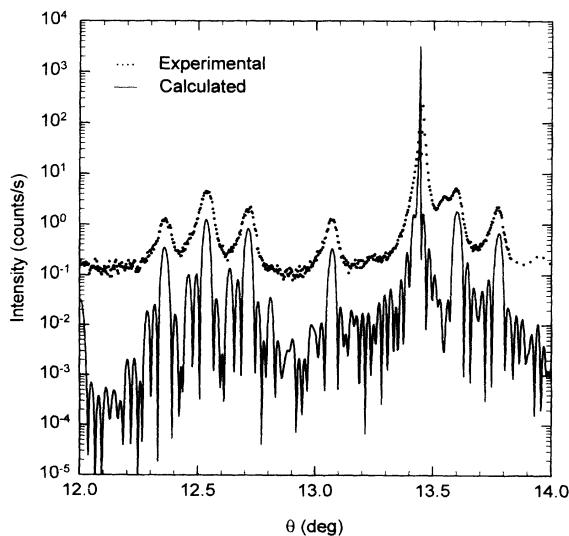


FIG. 2. A θ - 2θ scan of sample *B* with the calculated curve. The intense peak at 13.45° is from the (400) reflection of the ZnTe buffer layer.

TABLE I. The layer combinations used for samples *B* and *C* in obtaining the fits.

Sample <i>B</i>		Sample <i>C</i>	
9.0 layers MnTe	} 3 periods	4.0 layers MnTe	} 3 periods
9.5 layers ZnTe		8.0 layers ZnTe	
9.0 layers MnTe		4.5 layers MnTe	
10.0 layers ZnTe		8.5 layers ZnTe	

were perfectly coherent for only a few periods. Within those three periods it was found that by changing the order or choosing different combinations of layers (sometimes nine atomic bilayers, sometimes ten), the smallest peaks were greatly affected while the larger superlattice peaks remained largely unchanged. The combinations used to achieve the fits for sample *B* and sample *C* are shown in Table I. The larger superlattice peaks were primarily a function of the lattice parameters and layer thicknesses. Since the latter were of primary interest, no further refinement was attempted. The variable parameters and the results obtained are shown in Table II.

DISCUSSION

The calculated thickness of the superlattice as a whole exceeds the critical value. Using the theory developed by People and Bean,¹⁰ the calculated critical thickness of sample *B* was about 2000 \AA . But sample *B* had a superlattice thickness of about $1.2 \mu\text{m}$, which suggests that the superlattice is largely free of strain components resulting from the buffer layer. This was confirmed by observing that the buffer peak was not significantly displaced from its natural position. The calculated critical thickness for sample *C* was about 6000 \AA while its actual thickness was around 8000 \AA . Therefore this sample may still be somewhat strained due to the buffer. In contrast, because the thickness of the two layers within each cycle in the two superlattice samples is well below the critical thickness, interface matching occurs only through strain effects. Therefore the entire superlattice is pseudomorphic within itself, but free of strain from the buffer (at least for sample *B*).

The lattice parameter values obtained for ZnTe from the fitting results differ from the bulk value (6.100 \AA) in both samples. These results were used to calculate the vertical strain (ϵ_z). Using the Poisson ratio (ν) of ZnTe (0.363), the in-plane strain (ϵ_x) was calculated using the well-known relationship

$$\epsilon_x = -\epsilon_z \frac{(1-\nu)}{2}. \quad (1)$$

TABLE II. The variable parameters and the values used for both samples *B* and *C* in the fitting procedure.

Variable parameters (\AA)	Sample <i>B</i>	Sample <i>C</i>
lattice parameter (MnTe)	6.53	6.54
lattice parameter (ZnTe)	6.03	6.06
average layer thickness (MnTe)	58.77	27.80
average layer thickness (ZnTe)	58.83	50.00

From ϵ_x , the in-plane lattice parameter for ZnTe was determined. These calculations gave an in-plane lattice parameter value of 6.158 Å for sample *B*, and 6.135 Å for sample *C*. Assuming that the ZnTe in-plane lattice parameter values were also valid for MnTe (i.e., assuming pseudomorphic growth) and using the MnTe (400) lattice parameter value obtained from the fitting results, the strains were calculated for MnTe. The calculated values for the in-plane strain (ϵ_x) and the vertical strain (ϵ_z) for both samples are shown in Table III. It is immediately evident that MnTe undergoes a much higher strain than ZnTe, which suggests a surprising elastic behavior in the zinc-blende form of MnTe.

Neutron-diffraction experiments performed on sample *B* indicated the (400) MnTe lattice parameter as 6.50 ± 0.05 Å and the in-plane lattice parameter as 6.17 ± 0.05 Å (Ref. 11), which agree well with the present work.

The stress-strain relations for a cubic system with tetragonal distortion in the *z* direction are

$$X_x = C_{12}\epsilon_x + C_{11}\epsilon_x + C_{12}\epsilon_z, \quad (2)$$

$$Z_z = 2C_{12}\epsilon_x + C_{11}\epsilon_z = 0. \quad (3)$$

[Z_z is set to zero because the layers are unconstrained in the vertical (*z*) direction.]

Using the calculated strains (Table III) and the ZnTe elastic constants ($C_{11} = 7.13$, $C_{12} = 4.07$), Eq. (2) is used to solve for X_x . This is the in-plane shear force/area between the layers. To account for the differences in the layer thicknesses, X_x is multiplied by the ratio between the ZnTe and the MnTe layer thicknesses to determine the in-plane shear force/area acting on MnTe. Using the calculated strains for MnTe (Table III), Eqs. (2) and (3) are solved to determine the elastic constants of MnTe. The constants C_{11} and C_{12} for MnTe were calculated to be 2.22 and 1.16 for sample *B* and 2.08 and 1.01 for sample *C* (in units of 10^{11} dyn/cm²). The lower values for sample *C* are consistent with there being some residual strain between the buffer and the superlattice in that sample. The values for sample *B* are thus more trustworthy in this regard. The elastic constant C_{44} is related to a type of strain which was not present in these samples (lateral shear strain along 100 plane) and therefore could not be determined from this data.

Due to the strain dependence of the Poisson ratio and the elastic constants, there could be an inconsistency in using the unstrained values of these constants for ZnTe in Eqs. (1), (2), and (3). Although the elastic constants are generally strain dependent, the changes in them are negligible in the present work. The changes in the elastic constants can be expressed as a function of the strain and the

TABLE III. The calculated in-plane strains (ϵ_x) and the vertical strains (ϵ_z) for samples *B* and *C*.

Material	Sample <i>B</i>		Sample <i>C</i>	
	ϵ_x	ϵ_z	ϵ_x	ϵ_z
ZnTe	0.95%	-1.08%	0.57%	-0.66%
MnTe	-2.87%	3.00%	-3.23%	3.16%

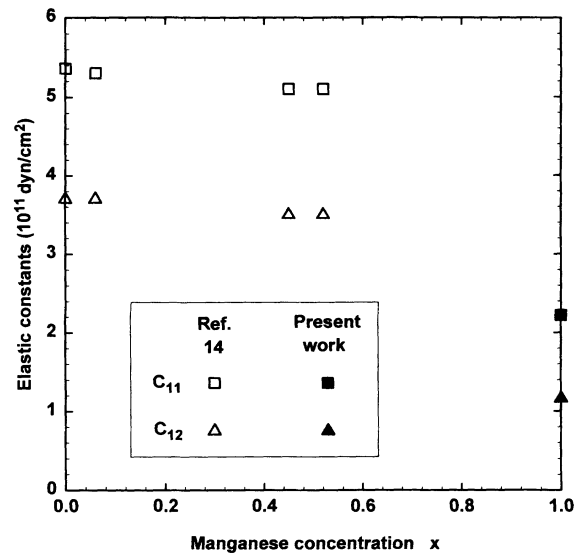


FIG. 3. Elastic constants C_{11} and C_{12} (in units of 10^{11} dyn/cm²) for alloys of $\text{Cd}_{1-x}\text{Mn}_x\text{Te}$ and the present results obtained for zinc-blende MnTe.

third-order elastic constants of the material.¹² Using the values for the third-order elastic constants,¹³ a 1% hydrostatic strain in ZnTe results in a 1.7% change in C_{11} and a 5.6% change in C_{12} . The change in the Poisson ratio would be only 2.5%. These changes would not effect the results significantly. Furthermore, the samples used for the present work are not under hydrostatic strain but under biaxial strain. They are free to contract or dilate in the *z* direction through the Poisson effect. Thus, the changes in this case would presumably be less than in the hydrostatic case. Therefore, the unstrained values of the

TABLE IV. The Poisson ratio and the bulk modulus values of some of the other materials along with the values found for zinc-blende MnTe. All values except for MnTe are taken from Ref. 16.

Material	C_{11}	C_{12} (10^{11} dyn/cm ²)	Bulk modulus	Poisson ratio
IV				
Si	16.57	6.39	9.78	0.278
Ge	12.89	4.83	7.52	0.273
III-V				
GaAs	11.81	5.32	7.48	0.311
InSb	6.67	3.65	4.66	0.354
AlSb	8.94	4.43	5.93	0.331
II-VI				
ZnS	10.40	6.50	7.80	0.385
ZnSe	8.59	4.06	5.57	0.321
ZnTe	7.13	4.07	5.09	0.363
CdTe	5.35	3.68	4.24	0.408
HgTe	5.08	3.58	4.08	0.413
MnTe	2.22	1.16	1.51	0.343
I-VII				
CuCl	2.72	1.87	2.15	0.407

Poisson ratio and the elastic constants were used.

While the elastic constants of zinc-blende MnTe have not previously been determined, acoustic measurements¹⁴ have been made for alloys of $\text{Cd}_{1-x}\text{Mn}_x\text{Te}$ in the range in which natural bulk growth occurs. Figure 3 shows these results together with the present values. While the trend of lowering the elastic constants with increasing Mn content is evident in the acoustic work, these results are surprising in that they show a much more dramatic decrease.

The values of the elastic constants and the bulk modulus of some of the diamond and zinc-blende materials are compared in Table IV. It is clear that the bulk modulus of MnTe is very low in comparison to all except CuCl. It has been suggested by Martin¹⁶ that the low value of the CuCl bulk modulus is due to its ionicity being quite close to the critical value for the stability of the zinc-blende structure. But MnTe too has an ionicity close to this critical value¹⁷ (preferring the NiAs structure), which in part may explain the low values obtained from the present work.

Differences exist between the superlattice samples used for the present work and the bulk alloys and the other zinc-blende materials. The present samples were grown as thin layers by MBE, and the strains were measured on superlattices in which the MnTe layers were around 60 Å thick. Furthermore, there is a strong uniaxial strain (3%) present in these superlattice samples. So the elastic constants obtained from the present work might be expected to differ from the equilibrium values. Lee *et al.*¹⁸ failed to find such an effect in ZnSe which was epitaxially grown on GaAs. However, the samples they used were strained only 0.25%. It remains to be determined whether one of these explanations or a combination of them is

responsible for the surprising elastic behavior in the new zinc-blende form of MnTe.

CONCLUSION

The lattice parameter of zinc-blende MnTe grown by MBE was measured to be 6.343 Å, which is consistent with previous measurements and with extrapolations from bulk alloys. Elastic constants C_{11} and C_{12} of the zinc-blende form of MnTe were also determined. While these values agree with the general trend observed in acoustic measurements on alloys of a decrease in elastic constants with increasing Mn concentrations, the values are surprisingly low compared to the other zinc-blende materials (II-VI, III-V, or group IV) and much lower than would be expected by linear extrapolations from the acoustic data referred to above. Although some speculation could be made as to why the elastic constants are so low in this new zinc-blende form of MnTe, further research is needed to obtain an explicit description.

ACKNOWLEDGMENTS

This work was supported in part by the National Science Foundation MRG Grant No. DMR 8913706 and by the Great Lakes Cluster of Pew Science Program. The authors wish to thank Dr. Robert Buschert and Dr. Carl Helrich for fruitful discussions, and also the following for their involvement in this work: Mark Guengerich for assembling the diffractometer, Susan Lehman, Alan Burkholder, and Leonard Mast for the technical work, Jeremy Kropf for modifying and interfacing the diffractometer and for the early data collection, and Evert Vandeworp for coding the fitting program.

*Present address: Department of Physics, Pennsylvania State University, University Park, PA 16802.

¹L. A. Kolodziejski, R. L. Gunshor, A. V. Nurmikko, and N. Otsuka, *Acta Phys. Pol. A* **79**, 31 (1991).

²S. M. Durbin, J. Han, Sungki O, M. Kobayashi, D. R. Menke, R. L. Gunshor, Q. Fu, N. Pelekanos, A. V. Nurmikko, D. Li, J. Gonsalves, and N. Otsuka, *Appl. Phys. Lett.* **55**, 2087 (1989).

³M. Hovinen, A. Salokatve, and H. Asonen, *J. Appl. Phys.* **69**, 3378 (1991).

⁴M. Quillec, L. Goldstein, G. Le Roux, J. Burgeat, and J. Primot, *J. Appl. Phys.* **55**, 2904 (1984).

⁵R. A. Cowley, *Acta Crystallogr. Sec. A* **43**, 825 (1987).

⁶J. M. Vandenberg, R. A. Hamm, M. B. Panish, and H. Temkin, *J. Appl. Phys.* **62**, 1278 (1987).

⁷D. R. Yoder-Short, U. Debska, and J. K. Furdyna, *J. Appl. Phys.* **58**, 4056 (1985).

⁸D. W. Berreman, *Phys. Rev. B* **14**, 4313 (1976).

⁹F. Abeles, *Ann. Phys.* **5**, 596 (1950).

¹⁰R. People and J. C. Bean, *Appl. Phys. Lett.* **47**, 322 (1985); **49**, 229 (1986).

¹¹P. Klosowski, Ph.D. thesis, University of Notre Dame, 1992.

¹²F. Birch, *Phys. Rev.* **71**, 809 (1947).

¹³R. F. Singh and S. Singh, *Phys. Status Solidi B* **140**, 407 (1980).

¹⁴P. Maheswaranathan, R. J. Sladek, and U. Debska, *Phys. Rev.* **31**, 5212 (1985).

¹⁵J. K. Furdyna, *J. Appl. Phys.* **64**, R29 (1988).

¹⁶R. M. Martin, *Phys. Rev. B* **1**, 4005 (1970).

¹⁷A. Balzarotti, N. Motta, A. Kisiel, M. Zimnal-Starnawska, M. T. Czyzyk, and M. Podgorny, *Phys. Rev. B* **31**, 7526 (1985).

¹⁸S. Lee, B. Hilebrands, G. I. Stegeman, H. Cheng, J. E. Potts, and F. Nizzoli, *J. Appl. Phys.* **63**, 1914 (1988).